COBEM 2021 26th International Congress of Mechanical Engineering
November 22-26, 2021, Virtual Congress, Brazil

COB-2021-0322
SCRAMJET DESIGN FOR ATMOSPHERIC FLIGHT FROM 23 TO 30 KM

Guilherme Melo Chaves
Marcelo Serrano Zanetti
João Felipe de Araújo Martos
Universidade Federal de Santa Maria (UFSM). Departamento de Engenharia Mecânica. Av. Roraima, 1000. Cidade Universitária Camobi. CEP. 97105-900. Santa Maria/RS. Brazil
guilhermitomelo@gmail.com; marcelo.zanetti@ufsm.br, joaodearaujo@hotmail.com

George Santos Marinho
Pedro Paulo Batista de Araújo
Paulo Gilberto de Paula Toro
Universidade Federal do Rio Grande do Norte (UFRN). Centro de Tecnologia. Av. Senador Salgado Filho, 3000 - Campus Universitário, Lagoa Nova CEP 59.078-970 – Natal/RN - Brasil
gmarinho@ct.ufrn.br; araujo.projects@gmail.com, toro11pt@gmail.com

Abstract. *In 2019, Aerospace Engineering undergraduate students, from Universidade Federal de Santa Maria (Santa Maria/RS), started to develop research in hypersonic airbreathing propulsion. In this present work, theoretical-analytical methodology based on oblique shock wave, one-dimensional (Rayleigh) flow with heat addition and expansion wave (Prandtl-Meyer) coupled area ratio equations, considering calorically perfect gas (no real gas effects) and no viscous effects (no boundary layer) assumptions, are applied to preliminary scramjet design. A two-dimensional hydrogen powered generic scramjet, with mixed (external and internal) compression inlet, for a flight starting at the speed of 1723 m/s (corresponding to Mach number 5.84) at 23 km and ending at the speed of 2051 m/s (corresponding to Mach number 6.8) at 30 km, considering shock on-lip and shock on-corner conditions. The zeroth and the first laws of thermodynamics are used to estimate the airflow static temperature, T_3, while the energy conservation law is used to estimate the Mach number, M_3, at the combustion chamber entrance. The turning (deflection) angles of the compression section ramps are optimized by applying the constant total pressure (recovery) ratio across each incident oblique shockwave (Oswatitsch criterion adapted for hypersonic scramjet inlet). The scramjet engine operates as an (opened) Brayton thermodynamic cycle, then, the static pressure, at the scramjet trailing-edge, is the static pressure at a given flight altitude, and it provides the turning (deflection) angle of the expansion section ramp (trailing-edge). Airflow thermodynamic properties from leading-to-trailing edges as well as the uninstalled trust are presented for both cases.*

Keywords: *scramjet, supersonic combustion, hypersonic airbreathing propulsion*

1. INTRODUCTION

The hypersonic airbreathing propulsion system has been investigated, since the middle 1950's decade, in the main research institutes and universities around the world (Fry, 2004; Curran, 2001). In 2019, undergraduate students, from Aerospace Engineering, at the Universidade Federal de Santa Maria (UFSM, Santa Maria/RS), started to develop research in hypersonic airbreathing propulsion (Soares, 2020). Also, in 2020, the Universidade Federal do Rio Grande do Norte (UFRN, Natal/RN) aiming the capacity of undergraduate and graduate students in the aero-thermo-structural design of airbreathing propulsion based on supersonic combustion (scramjet) technology to be applied, in the flight of an aerospace vehicle, at hypersonic speed in the Earth dense atmosphere (up to 60 km altitude), for access to space, provided an extension course, named "Preliminary design of an aerospace vehicle integrated with hypersonic airbreathing propulsion (scramjet technology) for flight in the Earth's dense atmosphere at an altitude of 20 km in speed corresponding to Mach number 5.79".

In 2018, Graduate students from Graduate Program in Mechanical Engineering, at the UFRN, started to develop research in hypersonic airbreathing propulsion. A two-dimensional generic hydrogen-powered scramjet was designed using an engineering approach, to demonstrate, during atmospheric flight, supersonic combustion, of the atmospheric air with hydrogen in supersonic speed, when the scramjet vehicle was flying at 2050 m/s (corresponding to Mach number 6.8) at an geometric altitude of 30 km. The oblique shock wave, one-dimensional compressible (Rayleigh) flow with heat addition, and the expansion wave (Prandtl-Meyer) coupled to the area ratio, considering calorically perfect gas and no viscous effects, were used to estimate the thermodynamic properties and velocities (Mach numbers) of supersonic airflow, from the leading-to-trailing edges of the scramjet vehicle. A generic scramjet, with three ramps in

the compression section, with deflection angles of 5.5^o, 7^o and 8.5^o, considering the constant total pressure recovery, and the same strength of incident shock waves, flying at 30 km of altitude with speed of 2051 m/s, was capable of generating supersonic speed corresponding to the Mach number of 2.55 and a static temperature of 1008 K, higher than 845.15 K, the ignition temperature, showing the possibility of burning hydrogen, at the combustion chamber. The combustion products were expanding, through the expansion deflection angle of 10°, to 2351.29 m/s, higher than the scramjet velocity of 2050 m/s, resulting positive (uninstalled) thrust, which indicated possibility to generate propulsion (Toro et al., 2018a; 2018b).

Later, an extension of this preliminary project, considering the optimization of the scramjet inlet based on the required static temperature and a given Mach number at the entrance of the combustion chamber and the required static pressure at the trailing-edge for a given fight atmospheric pressure condition was developed. Also, a boundary layer thickness from the leading-to-trailing edges of the vehicle was estimated and design modifications were proposed to accommodate it, such as the cowl repositioning, new compression ramp angles and the increase the height of the combustion chamber. The presence of the boundary layer modified the airflow's thermodynamic properties, representing an advantage to guarantee the auto-ignition of the fuel in the combustion chamber. However, it reduced the propulsive capacity of the vehicle by decreasing the combustion products flow velocity at the scramjet trailing-edge (Carneiro, 2020, Carneiro et al., 2020).

In 2020, the same procedure and strategies were applied to design a scramjet flying at 1710 m/s, in altitude of 20 km. Theoretical analytical (oblique shock wave, heat addition in one-dimensional compressible (Rayleigh) flow, and the expansion wave (Prandtl-Meyer) coupled to the area ratio, considering calorically perfect gas and no viscous effects) was applied to design a scramjet with power-on, burning hydrogen (Fernandes Filho et al., 2020). In this article no thrust was presented. At the same flight conditions, a numerical (CFD) was applied to design a scramjet with power-off, without injection or burning any fuel (Carvalho et al., 2020).

In the present article, the aerospace scramjet vehicle design, from the leading-to-trailing edges, with mixed (external and internal) compression configuration, was developed to fly from the speed of 1723 m/s (corresponding to Mach number 5.84) at 23 km and ending at the speed of 2051 m/s (corresponding to Mach number 6.8) at 30 km. The static temperature (T_3) and Mach number (M_3) conditions at the entrance of the combustion chamber, needed to burn the fuel (hydrogen) spontaneously in supersonic airflow velocity, considering calorically perfect gas (no real gas effects), inviscid flow (no boundary layer effects) and no spillage flow (shock on-lip and shock on-corner), was considered. The turning angles of compression ramps and the corresponding airflow thermodynamic property (pressure, temperature and density) ratios as well as the airflow velocities (and corresponding Mach numbers) are obtained based on all incident oblique shock waves are of equal strength (the normal component of the Mach number, which approach of each the incident oblique shock wave, is equal), adapted Oswatitsch criterion for hypersonic scramjet inlet.

2. SCRAMJET AND CHARACTERISTICS

An aerospace vehicle flying in a dense Earth atmosphere (up to 60 km altitude) at hypersonic speed, corresponding to Mach number, greater than 5 times the speed of sound, at flight altitude, using an airbreathing propulsion system based on supersonic combustion is called, simply, as scramjet. A scramjet (acronym of supersonic combustion ramjet) is an aeronautical airbreathing propulsion system, where the airflow, from the leading-to-trailing edges of the aerospace vehicle, remains supersonics, or greater than the speed of sound for a given static local temperature.

Observing the energy conservation law, the total temperature (enthalpy) is a function of the squared power of velocity. Consequently, due to the high-temperature environment, of the hypersonic airflow, the scramjet vehicles must have no moving parts. Therefore, the own scramjet inlet fixed geometry has to pressurize and decelerate the airflow, to the adequate conditions at the scramjet combustion chamber entrance capable to burn with the fuel at supersonic velocity. Also, the shock waves established in the compression (inlet) section of the scramjet must provide supersonic speeds at the entrance of the combustion chamber. Only, an aerospace vehicle with the wedge/conical form geometry, in supersonic/hypersonic velocity, establishes a plane (wedge) or conical oblique shockwave capable to pressurize and decelerate the supersonic/hypersonic airflow to supersonic velocity, at the entrance of the combustion chamber. Finally, in hypersonic velocity, the airflow has enough internal energy sufficiently high capable to start the dissociation/ionization of airflow (oxygen and nitrogen) molecules/atoms (Heiser and Pratt, 1994).

Due to scramjet must have no moving parts, scramjet is a highly integrated system, where the hypersonic airbreathing propulsion system and vehicle are indistinguishable. Therefore, scramjets are unable to produce thrust while stationary. Consequently, another propulsion system has to accelerate the scramjet to operate the supersonic combustion, at the combustion chamber, at flight conditions. Rocket engines may provide an affordable path for maturing hypersonic airbreathing components and subsystems in flight, and accelerate the scramjet to speed conditions, such that the shock waves established at the scramjet inlet be able to compress the atmospheric air achieving the operational conditions (Hass et al., 2005).

To better understand the features of the scramjet design, conventional terminology may be used. The scramjet operates according to (opened) Brayton thermodynamic cycle (Fig. 1) and may be divided into three main components

(Fig. 2): external and internal compression section (inlet), combustion chamber (combustor), and internal and external expansion section (outlet) (Heiser and Pratt, 1994).

The plane symmetrical scramjet (Fig. 2) consists of a two-wedge-derived waverider, symmetrical by a plane that passes through the leading-to-trailing edges, which each symmetrical part is a wedge-derived waverider.

Stations 0 and 1 are the scramjet and the cowl leading-edges, respectively (Fig. 2). Stations 3 and 4 are the entrance and exit of the combustion chamber, respectively (Fig. 2). Fuel is injected between the stations 3 and 4 (Fig. 2), at constant pressure (Fig. 1). Stations 9 and 10 are the cowl and the scramjet trailing-edges, respectively (Fig. 2). The combustion products are expanded directly into the Earth's atmosphere at atmospheric pressure at a given flight altitude, station 10 (Fig. 1), defining the opened thermodynamic process (Heiser and Pratt, 1994).

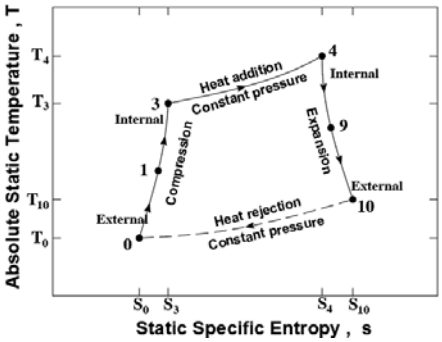

Figure 1. Brayton thermodynamic cycle of scramjet vehicles, adapted from Heiser and Pratt (1994).

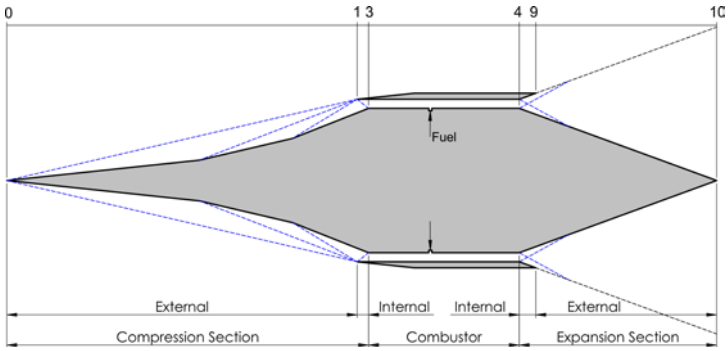

Figure 2. Plane symmetrical scramjet components and terminology, adapted from Heiser and Pratt (1994).

Basically, there are three scramjet inlet configurations. Mixed external and internal compression system, which is characterized by all incident oblique shock waves converge to the cowl leading-edge (shock on-lip), and the only one reflected shock wave converges to the combustion chamber entrance (shock on-corner) (Fig. 2).

In the external compression system, all incident oblique shock waves converge to the cowl leading-edge (shock on-lip), there is no reflected shock wave and the streamlines those experiments the last incident shock wave is aligned to the combustion chamber surfaces. The symmetrical internal compression system employs an additional surface, in order to generate a mirror-image of only one incident oblique shock wave, in each side, converging at the leading-edge of the (virtual) cowl (shock on-lip) and the odd reflected shock waves, where the last one converges to the entrance of the combustion chamber (shock on-corner) (Heiser and Pratt, 1994).

The external, stations 0 to 1, and internal, stations 1 to 3 (Fig. 2), at the adiabatic compression (inlet) section (Fig. 1) are governing by the incident and reflected plane oblique shock wave (Fig. 3) (Anderson, 2003). The combustion chamber section may be divided by constant area and constant pressure isolator, from the entrance, station 3, to fuel injection, and constant pressure supersonic combustion, from fuel injection to exit, station 4 (Fig. 1). The isolator is used to uniformize the flow from the compression section, and, in general, fuel is injected right after the isolator. The burning of hydrogen with the supersonic airflow at the combustion chamber is analytically simulated by the one-dimensional with heat addition (Rayleigh) flow theory (Fig. 3) (Anderson, 2003). The internal, stations 4 to 9, and external, stations 9 to 10 (Fig. 2), adiabatic expansion (outlet) section (Fig. 1) are governing by expansion wave (Prandtl-Meyer) flow theory coupled to area ratio theory (Fig. 3) (Anderson, 2003). The combustion products are expanded directly into the Earth's atmosphere at atmospheric pressure at a given flight altitude, station 10 (Fig. 2), opened thermodynamic process (Fig. 1) (Heiser and Pratt, 1994).

As mentioned early, an important feature of the scramjet is a highly integrated system, where the propulsion system and vehicle are indistinguishable. This tight integration is caused by the fact that the frontal (compression) section of the

vehicle contributes to the compression of atmospheric air, while the rear (expansion) section contributes to the generation of thrust (Figs. 2 to 3). The net thrust produced by the scramjet is the difference between the thrust (the force that propels the vehicle), generated by the expansion of exhaust gases from the rear of the scramjet, and the total drag (the force that resists the movement of the vehicle). These forces may produce thrust to the scramjet flight or not depending on the balance of these forces in scramjet vehicle design.

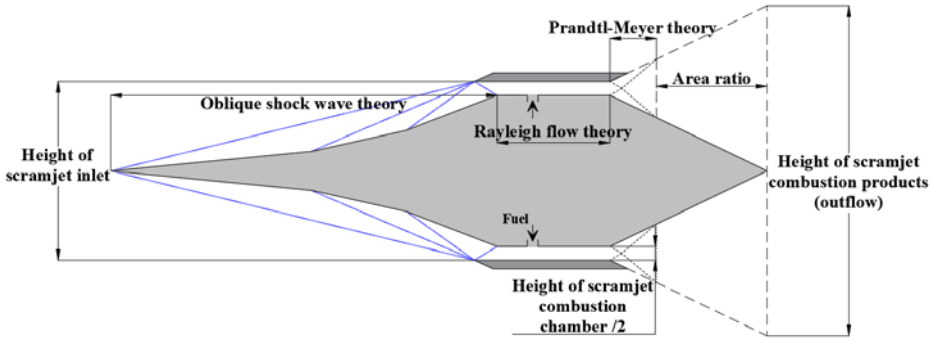

Figure 3. Two-Dimensional generic scramjet and analytical theories used (Carneiro, 2020).

Only, airbreathing propulsion system based on supersonic combustion is capable to provide the net (installed) thrust for efficiently hypersonic flight into the dense Earth atmosphere. The performance, measured in specific impulse (thrust per kilogram of fuel consumed), of an aerospace vehicle using airbreathing propulsion (turbine, ramjet or scramjet), with hydrocarbon or hydrogen fuel, is greater than that of a rocket engine, with solid propulsion or liquid propulsion. At hypersonic speeds, a typical value for the specific impulse of an H_2-O_2 rocket engine (from the launch to Earth's orbit, with Mach number 26) is about 400s, while the specific impulse of an H_2 fueled scramjet is 3000s to 500s, considering Mach numbers from 6 to 20, only up to 60 km altitude. Therefore, hydrogen, due to the fast time of ignition and high specific impulse, is the only aerospace fuel capable to provide a positive net thrust for sustained atmosphere flight at Mach numbers up to 20 (Fry, 2004). In addition to the scramjet having a higher specific impulse, it does not carry the oxidizer onboard, reducing vehicle weight, providing an advantage over rocket engines.

The scramjet design must fly at the constant dynamic pressure trajectory, as the space shuttle missions. Flying at higher dynamic pressure than 96000 Pa means the scramjet will be too heavy, required larger structural material thickness, for sustained atmosphere flight, while, for lower dynamic pressure than 23000 Pa, the scramjet will need a large wing area (Heiser and Pratt, 1994).

3. METHODOLOGY

3.1 Governing equations for theoretical analysis to design scramjet

In the analytical theoretical analysis, the subscripts *in* and *out* are used to identify the upstream (inlet) and the downstream (outlet) conditions, respectively, of each station (Fig. 7) of the generic scramjet inlet baseline.

Oblique shock wave (compression section, Fig. 3): Applying the mass, momentum and energy conservation laws, considering two-dimensional steady state, compressible flow, non-viscous effects, no heat conduction, and for calorically and/or thermally perfect gas ($p = \rho RT$, $\gamma = \text{constant}$) the oblique shock relationships can be easily obtained as closed form of the shock wave angle β, Mach number across the oblique shock wave, and the thermodynamic property (static pressure, static density and static temperature) ratios (Anderson, 2003), given by:

$$tg\theta_s = 2\left(\text{cotg}\,\beta\right)\left[\frac{\left(M_{in}\ sen\beta\right)^2 - 1}{M_{in}^2\left(\gamma + \cos 2\beta\right) + 2}\right] \qquad M_{out} = \left[\frac{1}{sen\left(\beta - \theta_s\right)}\right]\sqrt{\frac{\left(M_{in}\,sen\beta\right)^2 + \frac{2}{(\gamma-1)}}{\frac{2\gamma}{(\gamma-1)}\left(M_{in}\,sen\beta\right)^2 - 1}} \tag{1}$$

$$\frac{p_{out}}{p_{in}} = 1 + \frac{2\gamma}{(\gamma+1)}\left[\left(M_{in}\,sen\beta\right)^2 - 1\right] \qquad \frac{\rho_{out}}{\rho_{in}} = \frac{(\gamma+1)\left(M_{in}\,sen\beta\right)^2}{\left[(\gamma-1)\left(M_{in}\,sen\beta\right)^2 + 2\right]} \qquad \frac{T_{out}}{T_{in}} = \frac{\frac{p_{out}}{p_{in}}}{\frac{\rho_{out}}{\rho_{in}}}$$

where: ρ, p, T are density, pressure, and temperature of the gas, respectively, function of the incoming local supersonic/hypersonic flow Mach number M_{in}, the gas from the atmosphere γ (air in the Earth's planet, $\gamma = 1.4$) and the oblique shock wave β. For a given deflection (turning) angle θ_s the oblique shock wave β may be obtained iteratively with the relationship $\theta - \beta - M$. Note, the flow across the oblique shock wave promote an increase of pressure, density, temperature, and a decrease of Mach number, however the flow remains supersonic/hypersonic and parallel to the flat surface of the external compression section (Fig. 3).

One-Dimensional (Rayleigh) Flow with Heat Addition (Combustion chamber section, Fig. 3): Mass, momentum and energy conservation laws may be applied to the one-dimensional (Rayleigh) flow with constant-area heat addition (Anderson, 2003) to account for the combustion processes between the entrance (inlet) and the exit (outlet) of the scramjet combustor (Fig. 3). The energy equation q indicates the heat addition change the total energy (temperature). For calorically and/or thermally perfect gas, and applying the total temperature definition T_o, closed form of the thermodynamics property (static pressure, static density and static temperature) ratios across constant-area heat addition may be obtained (Anderson, 2003).

$$q = c_p\left(T_{o,out} - T_{o,in}\right) \qquad \frac{T_o}{T} = 1 + \frac{\gamma - 1}{2} M^2 \tag{2}$$

$$\frac{p_{out}}{p_{in}} = \left(\frac{1 + \gamma M_{in}^2}{1 + \gamma M_{out}^2}\right) \qquad \frac{\rho_{out}}{\rho_{in}} = \left(\frac{1 + \gamma M_{out}^2}{1 + \gamma M_{in}^2}\right)\left(\frac{M_{in}}{M_{out}}\right)^2 \qquad \frac{T_{out}}{T_{in}} = \frac{\frac{p_{out}}{p_{in}}}{\frac{\rho_{out}}{\rho_{in}}}$$

Note the flow from the external and internal compression section are deflected to the combustor entrance (Fig. 3) at supersonic speed (at constant pressure, constant density, constant temperature and constant Mach number). Fuel (H_2) will be injected right after the entrance station (Fig. 3) in (minimal) sonic speed. Rayleigh flow (one-dimensional flow with heat addition) may be applied to the combustion process to burn H_2 and O_2 in supersonic speed, resulting at the exit of the combustor chamber (outlet) an increase in static pressure, static density, static temperature, reducing the Mach number.

Prandtl-Meyer and area ratio (expansion wave section, Fig. 3). At the end of the combustion chamber, the streamlines find a deflection angle, according to the Prandtl-Meyer theory establishing a head of the expansion wave (**Figs. 3**). If the upper and lower surfaces of the combustion chamber have the same deflection angles, two heads of the expansion waves are established, which intersect equidistantly and establish two reflected heads of the expansion waves. These reflected waves reach the expansion surfaces and define a region where Prandtl-Meyer may be used (Fig. 3). After the two reflected heads of the expansion waves, the area ratio theory (Eq. 4) should be used (Heiser and Pratt, 1994). Once Mach number after expansion wave M_{out} the thermodynamic property (static pressure, static density and static temperature) ratios may be determined by the closed form given by the isentropic relationships (Anderson, 2003).

$$\mu_{head} = \operatorname{arcsen}\left(\frac{1}{M_{in}}\right) \qquad \mu_{tail} = \operatorname{arcsen}\left(\frac{1}{M_{out}}\right) \tag{3}$$

$$\theta = \upsilon\left(M_{out}\right) - \upsilon\left(M_{in}\right) \qquad \upsilon(M) = \sqrt{\frac{\gamma+1}{\gamma-1}}\ tg^{-1}\sqrt{\frac{\gamma-1}{\gamma+1}\left[M^2 - 1\right]} - tg^{-1}\sqrt{M^2 - 1}$$

$$\frac{T_{out}}{T_{in}} = \left(\frac{1 + \frac{\gamma - 1}{2} M_{in}^2}{1 + \frac{\gamma - 1}{2} M_{out}^2}\right) \qquad \frac{p_{out}}{p_{in}} = \left(\frac{T_{out}}{T_{in}}\right)^{\frac{\gamma}{\gamma - 1}} \qquad \frac{\rho_{out}}{\rho_{in}} = \frac{\frac{p_{out}}{p_{in}}}{\frac{T_{out}}{T_{in}}}$$

where: μ_{head} and μ_{tail} are the head and tail of the expansion wave angles, respectively. θ is the deflection (turning) expansion wave angle. υ (M) is the Prandtl-Meyer function.

$$\frac{A_{out}}{A_{in}} = \frac{M_{in}}{M_{out}} \left(\frac{1 + \frac{\gamma - 1}{2} M_{out}^2}{1 + \frac{\gamma - 1}{2} M_{in}^2} \right)^{\frac{\gamma+1}{2(\gamma-1)}} \tag{4}$$

Note the flow across the expansion wave (Prandtl-Meyer and area ratio) promote a decrease of static pressure, static density, static temperature, and an increase of Mach number. The flow remains supersonic/hypersonic and parallel to the flat surface of the internal and external expansion section (Fig. 3) of the hypersonic vehicle with airframe-integrated scramjet engine lower surface.

3.2 Scramjet inlet design by total pressure recovery

In 1944, Oswatitsch (1944) proposed an optimization criterion based on the maximum pressure recovery to minimize the possible losses applied to a problem of the intake of air for missiles flying at high supersonic speeds. Later, in 2015, Ran and Mavris (2005) applied the Oswatitsch criteria for a 2D mixed compression, two-ramp supersonic inlet, to maximize total pressure recovery, aiming the determination of the 2D supersonic inlet dimensions, matching the mass flow demand of the engine. The optimization criterion was applied for a system of (n-1) oblique shocks and one normal shock in two dimensions, where the maximum shock pressure recovery is obtained when the shocks are of equal strength. Toro et al. (2018c) modified the Oswatitsch optimization criterion developed by Ran and Mavris (2005), for a 2-D supersonic inlet, and applied to hypersonic scramjet inlet, a two-dimensional mixed (external and internal) compression system (Fig. 2), considering air as a calorically perfect gas and no boundary-layer effects. The total pressure recovery is presented by Heiser and Pratt (1994) as a parameter π (Eq. 5), and the maximum shock pressure recovery is obtained when the shock waves are of equal strength, i.e., the Mach numbers perpendicular to the individual shock waves are equal (Eq. 6).

$$\pi = \frac{p_{te}}{p_{ti}} = \frac{p_e}{p_i} \left[\frac{\left(1 + \frac{\gamma - 1}{2} M_e^2\right)}{\left(1 + \frac{\gamma - 1}{2} M_i^2\right)} \right]^{\frac{\gamma}{\gamma-1}} \tag{5}$$

$$M_1 sen\beta_1 = M_2 sen\beta_2 = ... = M_{n-1} sen\beta_{n-1} \tag{6}$$

3.3 Scramjet combustion chamber entrance conditions

The zeroth and the first thermodynamic laws and the energy conservation law, in term of total temperature T_t, are used to estimate the static temperature T_3 (Eq. 7) and Mach number M_3 (Eq. 8), respectively, at the combustion chamber entrance (Fig. 2) (Batista Araujo et al., 2021).

$$T_3 = \frac{\dot{m}_{fuel}}{\dot{m}_{air}} \frac{c_{p_{fuel}}}{c_{p_{air}}} \left(T_{fuel}^{ig} - T_{fuel}^{inj} \right) + T_{fuel}^{ig} \qquad \dot{m}_{air} = \rho_0 u_0 A_0 \qquad \dot{m}_{fuel} = f_{st}\, \dot{m}_{air} \qquad f_{st} = 0.0291 \tag{7}$$

$$M_3 = \sqrt{\frac{2}{\gamma - 1} \left\{ \left[\left(1 + \frac{\gamma - 1}{2} M_0^2\right) \frac{T_0}{T_3} \right] - 1 \right\}} \tag{8}$$

where: M_0, M_3, T_0, and T_3 are, respectively, the Mach numbers and static temperatures under freestream (flight velocity of the scramjet at a given geometric altitude) and the combustion chamber entrance conditions. $\dot{m}_{air}$ and $\dot{m}_{fuel}$ are the mass flow rate of atmospheric air and fuel, respectively. f_{st} is the stoichiometric fuel/air mass flow ratio determined by the atomic weights of the constituent elements.

4. RESULTS AND COMMENTARIES

The UFSM scramjet was designed to fly from (geometric) altitude of 23 km to 30 km, with hypersonic velocities from 1723 m/s to 2051 m/s, respectively. Therefore, it is necessary to define the thermodynamic atmospheric air properties for these conditions (Tab. 1).

Table 1. Thermodynamic atmospheric properties at 23 km and 30 km altitude, and flight conditions.

Thermodynamic atmospheric properties (U.S. Standard Atmosphere, 1976)						Flight conditions	
Altitude	Temperature	Pressure	Density	Sound speed		Velocity	Mach number
km	K	Pa	kg/m^3	m/s		m/s	
23	219.6	3467	0.05500	297.1		1723	5.8
30	226.5	1197	0.01841	301.7		2051	6.8

In both flight conditions (Tab. 1) the scramjet was designed with three compression ramps, with the turning (deflection) angles (Tab. 2) considering maximum total pressure recovery (Eq. 5) and all incident shock waves are of equal strength (Eq. 6), where in each case, the shock on-lip (all incident shock converged to the cowl leading-edge) and shock on-corner (the only reflected shock converged to combustion chamber entrance) conditions were guaranteed (Figs. 2 and 3), satisfying the combustion chamber entrance conditions (Tab. 3) of T_3 (Eq. 7) and M_3 (Eq. 8).

Table 2. Deflection angles and combustion chamber entrance conditions for scramjet at 23 km and 30 km altitude.

	θ_1	θ_2	θ_3		T_3	M_3
23 (km) / speed 1723 m/s (Mach 5.8)	7.25º	8.6º	10.3º		1024.76	1.81
30 (km) / speed 2051 m/s (Mach 6.8)	6.282º	7.427º	8.84º		1092.12	2.37

The $\theta - \beta - M$ relation (Eq. 1) was applied to obtain the incident oblique shockwave angles as well as the reflected oblique shockwave angle. Following, the thermodynamic air properties after each event may be evaluated by the thermodynamic property ratio (Eq. 1) and the freestream thermodynamic properties (Tab. 1). The Mach number after each incident and reflected shockwave may be evaluated by Eq. 1 (Tab. 3).

For no hydrogen-air combustion, the generic scramjet, with three ramps at the compression section (Figs. 2-3), with leading-edge angle of 7.25º, followed by two deflection angles of 8.6º and 10.3º, flying at 23 km of geometric altitude with speed 1723 m/s corresponding at Mach number 5.8 is capable to generate a supersonic velocity corresponding to Mach number of 1.81 and a static temperature of 1024.76 K, higher than 845.15 K, ignition temperature of hydrogen, at the entrance of combustion chamber. Consequently, it is possible to demonstrate a supersonic combustion when hydrogen may burn the supersonic atmospheric air, at the combustion chamber, during the atmospheric hypersonic flight of this generic scramjet. Considering no hydrogen-air combustion, the combustion chamber exit presented the same the combustion chamber entrance. At the expansion section, considering the airflow confined region the Prandtl-Meyer expansion theory was applied and after the area ratio was applied for the expansion ramp angle of 10º (Tab. 3).

Considering scramjet flying at 30 km in 2051 m/s (Mach 6.8) similar results were determined, considering leading-edge angle of 6.282º, followed by two deflection angles of 7.427º and 8.84º (Tab. 4).

Table 3. Thermodynamic properties at the generic scramjet, altitude 23 km, flight velocity 1723 m/s. Power-off.

		Station 0	1ª ramp	2ª ramp	3ª ramp	Reflection	Entrance	exit	Station 10
M_{in}	-	5.80	5.80	4.87	4.04	3.3	1.81	1.81	1.81
θ	º	-	7.25	8.6	10.3	26.15	-	-	-
β	º	-	15.37	18.4	22.35	43.45	-	-	-
M_{in} sen β	-	-	1.54	1.54	1.54	2.27	-	-	-
M_{out}	-	-	4.87	4.04	3.30	1.81	1.81	1.81	5.74
p_{out}/p_{in}	-	-	2.59	2.59	2.59	5.83	-	1.00	0.00486
T_{out}/T_{in}	-	-	1.35	1.35	1.35	1.92	-	1.00	0.21831
ρ_{out}/ρ_{in}	-	-	1.93	1.93	1.93	3.04	-	1.00	0.02227
p	Pa	3466.9	8984.82	23276.07	60312.95	351648.63	351648.63	351648.63	1709.51
T	K	219.57	295.41	397.38	534.59	1024.76	1024.76	1024.76	223.72
ρ	kg/m^3	0.05501	0.10596	0.20406	0.39305	1.19546	1.19546	1.19546	0.02662
a	m/s	297.04	344.54	399.61	463.50	641.72	641.72	641.72	299.84
u	m/s	1723.00	1677.93	1614.43	1529.54	1161.52	1161.52	1161.52	1720.07
T	K	1697.08	1696.63	1694.55	1698.94	1696.21	1696.21	1696.21	1696.21

Note, the supersonic airflow across the oblique attached (incident and reflected) shockwave promoted an increase of thermodynamic properties (pressure, temperature, density, and speed of sound) and a decrease of flow velocity (Mach number), and the streamline of the airflow remains supersonic and parallel to the flat surface (Tab. 3) of the generic scramjet compression section. Also, pressure ratio, temperature ratio, density ratio as well as the product M_{in} sen β are constant for all incident shock waves, characteristics of same shock strength. Also, the flow across the expansion wave and area ratio, promoted a decrease of thermodynamic properties (pressure, temperature, density, and speed of sound)

and an increase of flow velocity (and the correspondent Mach number). Finally, the total temperature from the leading-to-trailing edges is constant, since there was no heat addition, means, no hydrogen-air combustion. Therefore, the airflow velocity is slight lower than the flight scramjet condition, 23 km, 1723 m/s, and Mach number 5.8 (Tab. 3) and corresponding results for 30 km, 2051 m/s and Mach number 6.8 (Tab. 4).

Table 4. Thermodynamic properties at the generic scramjet, altitude 30 km, flight velocity 2051 m/s. Power-off.

		Station 0	1ª ramp	2ª ramp	3ª ramp	Reflection	Entrance	exit	Station 10
M_{in}	-	6.80	6.80	5.737872	4.80293	3.97	2.372104	2.37	2.37
θ	^{o}	-	6.282	7.427	8.84	22.549	-		
β	^{o}	-	13.14221	15.63131	18.77737	35.54302	-		
M_{in} sen β	-	-	1.55	1.55	1.55	2.31	-		
M_{out}	-	-	5.74	4.80	3.97	2.37	2.37	2.37	6.66
p_{out}/p_{in}	-	-	2.62	2.62	2.62	6.05	-	1.00	0.00463
T_{out}/T_{in}	-	-	1.35	1.35	1.35	1.95	-	1.00	0.21534
ρ_{out}/ρ_{in}	-	-	1.94	1.94	1.94	3.10	-	1.00	0.02152
p	Pa	1197	3138.76	8229.75	21577.47	130593.86	130593.86	130593.86	605.16
T	K	226.5	306.04	413.49	558.66	1092.12	1092.12	1092.12	235.18
ρ	kg/m^3	0.018411	0.03573	0.06934	0.13456	0.41659	0.41659	0.41659	0.00896
a	m/s	301.70	350.69	407.63	473.82	662.48	662.48	662.48	307.42
u	m/s	2051.00	2012.21	1957.82	1881.85	1571.47	1571.47	1571.47	2047.28
T	K	2320.09	2321.17	2321.17	2321.17	2321.17	2321.17	2321.17	2321.17

Considering power-on, means hydrogen-air combustion at the combustion chamber section, the one-dimensional (Rayleigh) flow with heat addition was applied (Fig. 3), considering no viscous effects and the airflow behaves as calorically perfect gas. One may observe, the thermodynamic properties and airflow velocities (Mach number) at the compression section must be the same for power-off (no hydrogen-air combustion), for both cases, flight scramjet condition, 23 km, 1723 m/s, and Mach number 5.8 (Tab. 5) and corresponding results for 30 km, 2051 m/s and Mach number 6.8 (Tab. 6).

The flow across the heat addition in one-dimensional flow promoted a decrease of thermodynamic properties (pressure, density, temperature, and speed of sound), and an increase of flow velocity (and the correspondent Mach number), and the total temperature increase when heat was added in the supersonic airflow, and remains constant up to the trailing edge.

Table 5. Thermodynamic properties at the generic scramjet, altitude 23 km, flight velocity 1723 m/s. Power-on.

		Station 0	1ª ramp	2ª ramp	3ª ramp	Reflection	Entrance	exit	Station 10
M_{in}	-	5.80	5.80	4.87	4.04	3.3	1.81	1.81	1.1
θ	^{o}	-	7.25	8.6	10.3	26.15	-		
β	^{o}	-	15.37	18.4	22.35	43.45	-		
M_{in} sen β	-	-	1.54	1.54	1.54	2.27	-		
M_{out}	-	-	4.87	4.04	3.30	1.81	1.81	**1.1**	5.74
p_{out}/p_{in}	-	-	2.59	2.59	2.59	5.83	-	2.07	0.00178
T_{out}/T_{in}	-	-	1.35	1.35	1.35	1.92	-	1.59	0.16381
ρ_{out}/ρ_{in}	-	-	1.93	1.93	1.93	3.04	-	1.31	0.01086
p	Pa	3466.9	8984.82	23276.07	60312.95	351648.63	351648.63	729212.75	1297.32
T	K	219.57	295.41	397.38	534.59	1024.76	1024.76	1627.58	266.61
ρ	kg/m^3	0.05501	0.10596	0.20406	0.39305	1.19546	1.19546	1.56085	0.01695
a	m/s	297.04	344.54	399.61	463.50	641.72	641.72	808.74	327.32
u	m/s	1723.00	1677.93	1614.43	1529.54	1161.52	1161.52	889.61	1877.76
T	K	1697.08	1696.63	1694.55	1698.94	1696.21	1696.21	2021.46	2021.46

Table 6. Thermodynamic properties at the generic scramjet, altitude 30 km, flight velocity 2051 m/s. Power-on.

		Station 0	1ª ramp	2ª ramp	3ª ramp	Reflection	Entrance	exit	Station 10
M_{in}	-	6.80	6.80	5.737872	4.80293	3.97	2.37210399	2.37	1.10
θ	^{o}	-	6.282	7.427	8.84	22.549	-		

β	^{o}	-	13.14221	15.63131	18.77737	35.543017	-		
M_{in} sen β	-	-	1.55	1.55	1.55	2.31	-		
M_{out}	-	-	5.74	4.80	3.97	2.37	2.37	1.10	6.66
p_{out}/p_{in}	-	-	2.62	2.62	2.62	6.05	-	3.30	0.00071
T_{out}/T_{in}	-	-	1.35	1.35	1.35	1.95	-	2.34	0.12584
ρ_{out}/ρ_{in}	-	-	1.94	1.94	1.94	3.10	-	1.41	0.00562
p	Pa	1197	3138.76	8229.75	21577.47	130593.86	130593.86	430350.32	304.21
T	K	226.5	306.04	413.49	558.66	1092.12	1092.12	2550.28	320.92
ρ	kg/m^3	0.018411	0.03573	0.06934	0.13456	0.41659	0.41659	0.58788	0.00330
a	m/s	301.70	350.69	407.63	473.82	662.48	662.48	1012.35	359.12
u	m/s	2051.00	2012.21	1957.82	1881.85	1571.47	1571.47	1113.58	2391.54
T	K	2320.09	2321.17	2321.17	2321.17	2321.17	2321.17	3167.45	3167.45

The first station 0 corresponds to the temperature and velocity for 23km and 30 km, respectively (Fig. 4). The three incident shock waves are established at the three compression ramps (jumps 1st, 2rd and 3rd) due to the vehicle's external compression system. According to the shock wave theory, thermodynamic properties (pressure, temperature, density, and sound speed) must increase, while the airflow velocity (and corresponding Mach number) decreases. At the expansion section occurs just the opossite, thermodynamic properties must decrease, while the airflow velocity (Mach number) increases. The heat added in supersonic airflow must increased the thermodynamic properties and remains supersonic, higher than sound speed to avoid the chocking flow. In both cases, the temperature at the combustion chamber was higher than hydrogen ignition temperature of 845 K, while the velocity was in supersonic regime.

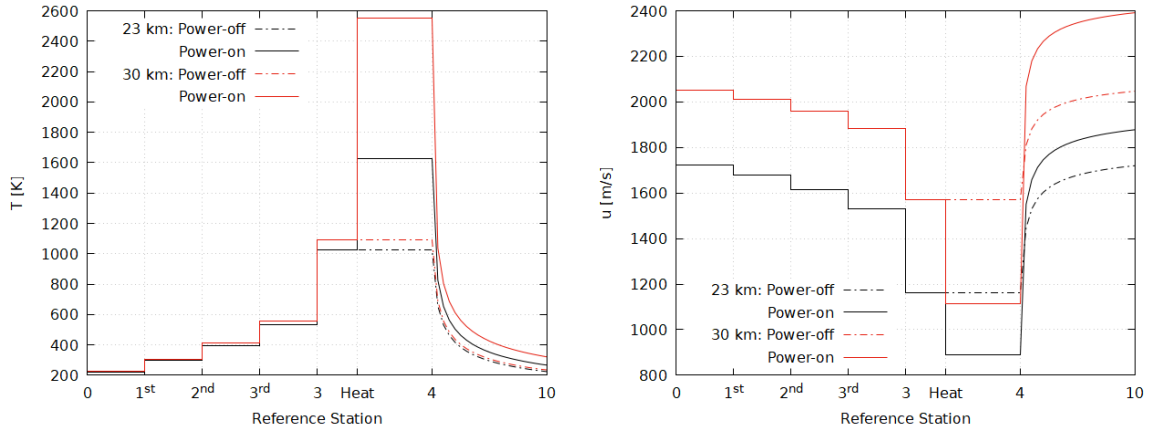

Figure 4. Temperature and velocity distribution from leading-to-trailing edges of generic scramjet.

5. CONCLUSIONS

A 2-D generic scramjet design is being developed at the Universidade Federal de Santa Maria (UFSM), to demonstrate in atmospheric flight the supersonic combustion, of atmospheric air (in supersonic speed) with hydrogen, in two flight conditions: 23 km, 1723 m/s, and Mach number 5.8 and 30 km, 2051 m/s and Mach number 6.8.

The main aspects of a scramjet design that obey the fundamental conservation laws of physics are explored. Oblique shock wave theory, one-dimensional (Rayleigh) flow with heat addition, and Prandtl-Meyer expansion wave coupled to area ratio were applied to obtain the thermodynamic properties (pressure, density, temperature, and speed of sound), and the airflow velocity (and the correspondent Mach number), to design the compression, combustor and expansion sections of the generic scramjet, respectively, considering no effects of boundary layer and calorically perfect gas airflow. Based on the temperature and Mach number at the combustion chamber entrance need to spontaneously ignition the hydrogen fuel, the turning (deflection) angles of the compression section ramps were obtained by applying the constant shock waves of equal strength that result in total pressure (recovery) ratio across each incident oblique shockwave, and shock on-lip and shock on-corner conditions.

For a given scramjet air inlet configuration the methodology presented in this work was capable of evaluating the thermodynamic properties and Mach numbers (corresponding to flow velocities) from the leading-to-trailing -edges of the generic scramjet.

Two scramjets configurations were analyzed, with mixed (external and internal) compression system configuration, with three ramps at the compression section, were analytically studied. First one, the scramjet inlet had leading-edge angle of 7.25^o, followed by two deflection angles of 8.6^o and 10.3^o, flying at 23 km of geometric altitude with speed 1723 m/s corresponding at Mach number 5.8. The second one considered scramjet flying at 30 km in 2051 m/s (Mach 6.8) with leading-edge angle of 6.282^o, followed by two deflection angles of 7.427^o and 8.84^o.

In both cases, the generic scramjet, with three ramps at the compression section, with the turning angles of 7.25^o, 8.6^o and 10.3^o, flying at 23 km in 1723 m/s (Mach 5.8), and with the turning angles of 6.282^o, 7.427^o and 8.84^o flying at 30 km in 2051 m/s (Mach 6.8) are capable to generate a supersonic velocity corresponding to Mach number of 1.81 and a temperature of 1024.76 K, and Mach number of 2.37 and a temperature of 1092.12 K, respectively, higher than the hydrogen ignition temperature of 845.15 K, showing the possibility to burn hydrogen-air mixture.

6. ACKNOWLEDGEMENTS

This study was financed in part by the Coordenação de Aperfeiçoamento de Pessoal de Nível Superior - Brasil (CAPES) - Finance Code 001. . Also, the authors would like to thank CAPES the support given by the Project PROCAD-DEFESA 88887.626266/2021-00. The authors would like to thank Universidade Federal de Santa Maria (UFSM) to support granted to carry out research on hypersonic airbreathing propulsion. Also, the three last authors would like to extend their gratitude to the Universidade Federal do Rio Grande do Norte (UFRN).

7. REFERENCES

Anderson Jr., J. D. (2003) Modern Compressible Flow: with Historical Perspective. McGraw-Hill series in Aeronautical and Aerospace Enginnering. Third Edition. ISBN O-07-242443-5. ISBN 0-07-1 12161-7 (ISE).

Carneiro, R., Aráujo, P. P. B., Borba, G. L., Marinho, G. S., Toro, P. G. P. (2020). Influence of the boundary layer on the design of the compression section of a generic scramjet. 18th Brazilian Congress of Thermal Sciences and Engineering. (ENCIT 2020-0805). Online.

Carneiro, R. (2020). Estudo analítico de um demonstrador da tecnologia da combustão supersônica. Dissertação de Mestrado. Programa de Pós-Graduação em Engenharia Mecânica. UFRN.

Carvalho, L., A., S., Santos, L., M., C., Fernandes Filho, J., Araújo, P. P. B., , Medeiros, J. B., Toro, P. G. P. (2020). Academic scramjet Design to flight at 20 km of altitude at Mach number 5.79 integrated at rocket engine S30. 18th Brazilian Congress of Thermal Sciences and Engineering. (ENCIT 2020-0547). Online.

Curran, E. T. (2001) Scramjet Engines: The First Forty Years. (AIAA) Journal of Propulsion and Power, 17(6), 1138–1148. doi:10.2514/2.5875

Fernandes Filho, J., Carvalho, L., A., S., Santos, L., M., C., Marinho, G. S., Medeiros, J. B., Toro, P. G. P. (2020). Preliminary design and analysis of a generic scramjet air for atmospheric flight at mach number 5.8. 18th Brazilian Congress of Thermal Sciences and Engineering. (ENCIT 2020-0649). Online.

Fry, R. S. (2004) A Century of Ramjet Propulsion Technology Evolution. (AIAA) Journal of Propulsion and Power, 20(1), 27–58. doi:10.2514/1.9178

Hass, N., Smart, M., & Paull, A. (2005). Flight Data Analysis of the HyShot 2. AIAA/CIRA 13th International Space Planes and Hypersonics Systems and Technologies Conference. doi:10.2514/6.2005-3354

Heiser, W.; Pratt, D.; Daley, D.; Mehta, U. (1994) Hypersonic Airbreathing Propulsion. AIAA Education Series. ISBN 1-56347-035-7. https://doi.org/10.2514/4.470356

Oswatitsch, K. (1947). Pressure Recovery for Missiles with Reaction Propulsion at High Supersonic Speeds (The Efficiency of Shock Diffusers). NACA Technical Memorandum 1140.

Ran, H.; Mavris, D. (2005). Preliminary design of a 2D supersonic inlet to maximize total pressure recovery. AIAA5th Aviation, Technology, Integration, and Operations Conference. Arlington, Virginia, USA.

Soares, L. H. S. M. (2020). Modelagem e implementação de ferramenta para projeto preliminar de motor hipersônico aspirado. Trbalho de Conclusão de Curso. Engenharia Aeroespacial. Universidade Federal de Santa Maria (UFSM).

Toro, P. G. P.; Carneiro, R.; Araújo, J. W. S.; Marinho, G. S.; Borba, G. L.; Rego, I. S.; Martos, J. F. A. (2018a). Design and Analysis of a generic scramjet air inlet. 17th Brazilian Congress of Thermal Sciences and Engineering (ENCIT 2018-0751). Águas de Lindóia/SP, Brazil.

Toro, P. G. P.; Carneiro, R.; Araújo, J. W. S.; Marinho, G. S.; Borba, G. L.; Rego, I. S.; Martos, J. F. A. (2018b). Design of the Generic Scramjet Combustion Chamber. 17th Brazilian Congress of Thermal Sciences and Engineering (ENCIT 2018-0056). Águas de Lindóia/SP, Brazil.

Toro, P. G. P.; Fernandes, A. G. L. N.; Marinho, G. S.; Borba, G. L.; Martos, J. F. A.; Rego, I. S.; (2018c). A new approach to optimize the scramjet inlet design applying the total pressure recovery. 17th Brazilian Congress of Thermal Sciences and Engineering (ENCIT 2018-0074). Águas de Lindóia/SP, Brazil.

U.S. Standard Atmosphere. (1976). NASA TM-X 74335. National Oceanic and Atmospheric Administration, National Aeronautics and Space Administration and United States Air Force.

8. RESPONSIBILITY NOTICE

The Authors are the only responsible for the printed material included in this scientific article.
The Authors declare that there is no conflict of interest regarding the publication of this scientific article.